Article

Parametric Optimization of NACA 4412 Airfoil in Ground Effect Using Full Factorial Design of Experiment

Shwe Yee Win[a] and Mongkol Thianwiboon[b,*]

Department of Industrial Engineering, Faculty of Engineering, Mahidol University, Nakhon Pathom 73170, Thailand

E-mail: [a]mayyeekhaingwin2481994@gmail.com, [b,*]mongkol.thi@mahidol.ac.th (Corresponding author)

Abstract. This investigation emphasizes the changes of the lift-to-drag ratio of an airfoil with the variation of ground clearance and angles of attack. Various ground clearances and angles of attack with a fixed speed of 30 m/s are applied to the NACA 4412 airfoil. Computational fluid dynamics (CFD) is used to calculate the aerodynamic coefficients acting on it. To study the influence of these two factors on the lift-to-drag ratio, 3^2 factorial design based on Design of Experiments (DOE) is utilized. A total of 9 numerical experiments were carried out with Ansys Fluent. When the angle of attack decreases, lift coefficient increases and drag coefficient decreases resulting in a high lift-to-drag ratio: also, the lower the ground clearance, the higher the lift-to-drag ratio. It shows the effectiveness of ground clearance and angle of attack. The analysis shows that either increasing ground clearance or using a higher angle of attack gives a decrement in the lift-to-drag ratio, but there is no interaction between them.

1. Introduction

Wing-In-Ground (WIG) craft is the official term for a kind of flying vehicle designed for efficient utilization of the ground effect (GE) in their whole operation [1]. They can take more cargo on board or more passengers which means that energy consumption by this aircraft per passenger is smaller than a traditional airplane [2]. They fly just above the ground, whether it is land or water. They exploit the ground effect behavior to increase lift and reduce drag. They are a unique class of high-speed, low-altitude transport vehicle [3]. This ground effect happens when air is trapped between the airfoil or wing and the landing surface and the distance between them is within limits [4]. In the literature, ground effect is defined in different ways. A clear definition is "a phenomenon of aerodynamic, aeroelastic and aeroacoustics impacts on platforms flying in close proximity to an underlying surface" [1]. This phenomenon has been known, at least, for the past 80 years [5]. Many researchers have studied the potential advantages of this phenomenon [1] to design safer and faster wings for ground effect vehicles. Since the 1960s, many related research topics have appeared and are still active [6].

In ground effect, one of the main parameters to consider is the ground clearance, which is the ratio of height divided by chord (H/C) [1]. The term height here refers to the distance between the ground surface and the trailing edge of the airfoil. Normally, the ground clearance is less than or equal to one-fifth of the chord length [7]. There is also a dependency on angle of attack. With positive angles of attack, a higher angle produces higher lift force until stall [1]. The angle at which relative wind meets an airfoil is the Angle of Attack (AoA) [8], as illustrated in Fig. 1. AoA can be simply described as the difference between where a wing is pointing and where it is going [1].
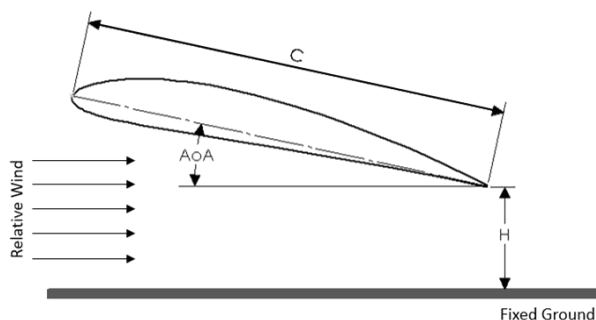

Fig. 1. Definition of AoA and Ground clearance.

Due to the ground effect, the flow around an airfoil is significantly changed and the aerodynamic characteristics also vary. The most important aerodynamic characteristics of the airfoil are the aerodynamic forces on it which are lift and drag. The force perpendicular to the motion of the airfoil is noted as lift and the force parallel to its motion is drag. The lift and induced drag are the components of the resultant force perpendicular and parallel to the velocity vector of the airfoil [7].

The friction of the moving object and air creates another form of drag, described as parasitic or profile drag. So, the total drag of a moving object across the air is the sum of induced drag and parasitic drag. The pitching moment is generated due to the aerodynamic forces acting on the airfoil and is calculated at the aerodynamic center, located at approximately 25% of the chord length [8].

There are many variables which affect both lift and drag, such as the density of air, the velocity of objects in the air, and the geometry of objects. Descriptions of non-dimensionalized lift, drag and moment are stated in terms of coefficient of lift (C_L), coefficient of drag (C_D) and coefficient of moment (C_M). In this way, lift, drag, and moment can be explained in terms of geometry alone and are independent of velocity or air density [3]. The ground effect greatly improves the behavior of the flow around an airfoil [4], so it is important to know the effective ground clearance.

Numerical studies and experiments were performed to study the ground clearance on various airfoils [9], [10], [11], [12], [13] and these studies concluded that an airfoil generates high lift and low drag when it is close enough to the ground. The dimensionless parameters named as ground clearance and angle of attack are varied to examine the effects of change in altitude on aerodynamic coefficient and lift-to-drag ratio of airfoils [12], [14], [15],[16]. The authors reported that the effect of the ground on the flow around an airfoil is modified as the split streamline and stagnation point move down at a positive angle of attack, the speed slows down and the pressure under the airfoil increases. Investigations were also conducted for various ground types such as long and short ground [17], fixed and moving ground [15]. Investigations about aerodynamic coefficients are never planned with the design of experimental methods.

In this paper, the effects of proximity to ground on aerodynamic characteristics of an NACA 4412 airfoil were studied. We calculated the aerodynamic coefficients by varying the ground clearance and AoA with the help of computational fluid dynamics (CFD). The variation is set up based on the 3^k full factorial design of experiments to study not only the effect of each parameter but also the interaction on the desired responses. When the required values were collected, ANOVA was used for analysis. By using the main effects plots, the more effective parameters which affect the aerodynamic efficiency can be identified. The optimized values of the two parameters can be obtained from regression with surface and contour plots.

2. Airfoil Geometry

Airfoil size and shape play an important role in efficiency of particular craft because wings are the surfaces that support the aircraft by means of dynamic reaction [18]. A section of a wing that is cut perpendicular to the wingspan is called an airfoil [8]. The NACA 4412 airfoil, which is a type of NACA four-digit airfoil was investigated to study the relationship between the ground effect and its

aerodynamic lift, drag and moment coefficient. The representation of the digits in the NACA 4412 airfoil can be seen in Table 1.

Table 1. Representation of the digits in NACA 4412 airfoil.

Maximum camber in percent chord	Position of maximum camber in tenths of chord length	Maximum thickness-to-chord ratio
4	4	12
maximum camber of 4 percent	40 percent of the chord length	maximum thickness of 12 percent of the chord

Table 2. NACA 4412 Coordinate points for airfoil profile.

	Upper Side		Lower Side	
S. No.	X	Y	X	Y
1	1.0000	0.0013	0.0125	-0.0143
2	0.9500	0.0147	0.0250	-0.0195
3	0.9000	0.0271	0.0500	-0.0249
4	0.8000	0.0489	0.0750	-0.0274
5	0.7000	0.0669	0.1000	-0.0286
6	0.6000	0.0814	0.1500	-0.0288
7	0.5000	0.0919	0.2000	-0.0274
8	0.4000	0.0980	0.2500	-0.0250
9	0.3000	0.0976	0.3000	-0.0226
10	0.2500	0.0941	0.4000	-0.0180
11	0.2000	0.0880	0.5000	-0.0140
12	0.1500	0.0789	0.6000	-0.0100
13	0.1000	0.0659	0.7000	-0.0065
14	0.0750	0.0576	0.8000	-0.0039
15	0.0500	0.0473	0.9000	-0.0022
16	0.0250	0.0339	0.9500	-0.0016
17	0.0125	0.0244	1.0000	-0.0013
18	0.0000	0.0000	-	-

The coordinate point for the NACA 4412 airfoil [19] as presented in Table 2 is used to generate the airfoil geometry shown in Fig. 2.
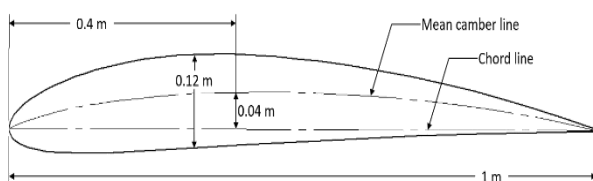

Fig. 2. NACA 4412 airfoil geometry.

3. Design of Experiments (DoE)

Design of Experiments (DoE) was first introduced for physical experiments with the aim of understanding the probabilistic behavior of agricultural crop systems at the beginning of the 20th century [20]. As a statistical research design tool, it has been using in many research areas [21],[22],[23],[24]. Since the designed experiments can clearly establish the relationship between the measured parameters of output (response) and the input variables (factors) and can answer questions about which factors are causing the majority of the response variability [22], DoE has become a part of parametric optimization and analysis [25]. It can also investigate the causes and effects of several different factors in a single study [22]. With the advent of numerical methods and computing facilities, it has been adapted in computer-based simulations [26],[27],[28]. The researcher designed the experiments statistically, to improve the efficiency of the experimentation, to avoid misleading conclusions and to reduce the number of runs or tests required.

3^k full factorial design of experiments with 2 factors generates a matrix of input parameters to characterize the flow behavior around the airfoil in ground effect. For 3^k factorial design, the factorial is arranged with k factors, each at three levels. Each factor is set to three levels: low, intermediate, and high. The number of runs is calculated as the factor of k, $3 \times 3 \times 3 \times \dots \times k$. So, it will be 9 ($3 \times 3 = 9$) or 3^2. In total, 9 cases using Computational Fluid Dynamics (CFD) simulations are calculated to compute the aerodynamic characteristics of the airfoil. As the research tends to investigate the flow behavior around the airfoil in ground effect, the ground clearance and angle of attack are chosen as input parameters and the lift-to-drag ratio and moment coefficient are considered as responses. Ground clearance is assigned as factor A with three levels, 0.1, 0.15 and 0.2, and the angle of attack is factor B. 4, 6 and 8 degrees. A total of 9 treatment combinations of 3^2 full factorial design used in this investigation is shown in Fig. 3. The numbers in Fig. 3 represent the experiments with the variation of two factors.
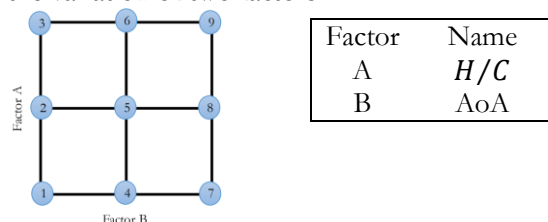

Factor	Name
A	H/C
B	AoA

Fig. 3. Treatment combinations in a 3^2 design.

4. Computational Experiment

Computational fluid dynamics (CFD) is used in the current research because it requires recognition of the physical phenomena that occur around the airfoil in order to calculate the aerodynamic force on the airfoil and improve its performance. A commercial CFD code Ansys Fluent of a realizable k-epsilon turbulence model covering the Navier-Stokes equations, and the finite volume

method was used for computing the aerodynamics coefficients of the NACA 4412 airfoil in ground effect with a fixed velocity of 30 m/s. This turbulence model is reasonable for many flows and is easy to implement. It is also stated to be the best turbulence model to simulate the flow pass an airfoil [29].

4.1. Boundary

The computational domain for the simulation is shown in Fig. 4. The setting of the boundary is based on the chord of the airfoil, C. The distance from the leading edge of the airfoil to the velocity inlet is 3.5C and from the trailing edge to the pressure outlet is 8C. The height from trailing edge to the upper wall is 4C. The ground clearance (H/C) of 0.1, 0.15, 0.2, indicate the height from the ground to the trailing edge. The dimensions of the boundaries are setup according to the Ansys manual [30] which confirmed that they are large enough not to have a measurable effect on the aerodynamic coefficients.
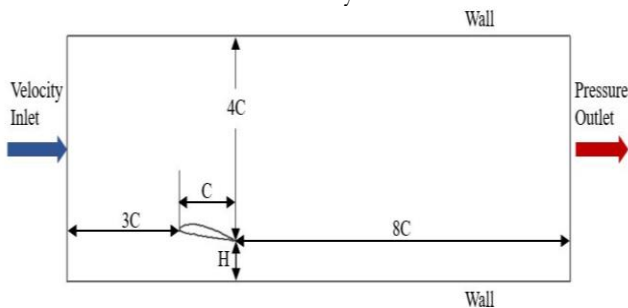
Fig. 4. Boundary Model Creation.

4.2. Meshing

A structured mesh is used for creating surface mesh all over the computational boundary. Quadrilateral dominant meshing is added apart from the area around airfoil. In addition, bias is applied for the smooth transition around the airfoil. To make a smooth mesh, an inflation with 1 mm first layer thickness is applied to the airfoil. The first layer thickness is calculated from the required y+ value for the k-epsilon model. So, the y+ value of the converged solution is maintained below 50 (y+ < 50). The geometry of the generated computational mesh is shown in Fig. 5 and a close-up of the meshing is shown in Fig. 6.
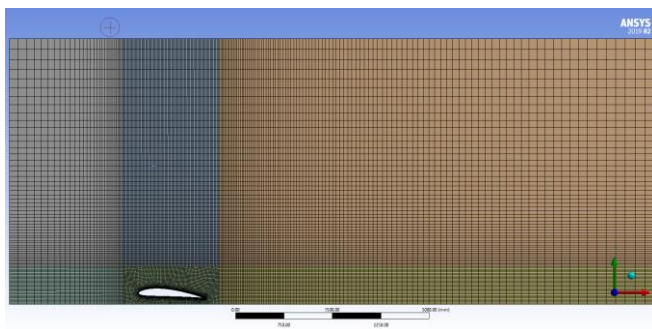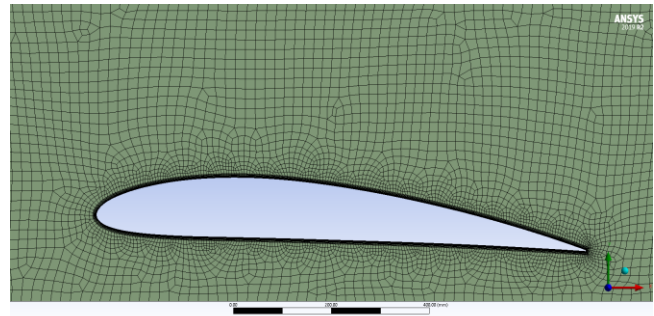
Fig. 5. Meshing Setup.

Fig. 6. Meshing Setup Close-up.

4.2.1 Mesh Sensitivity Study

In order to investigate whether a regularization scheme is able to realistically predict the aerodynamic characteristics for different element sizes, a mesh sensitivity study was carried out at 8 degrees AoA and 0.2 of ground clearance. Six types of mesh with different element numbers were used while other settings remained constant as shown in Table 3.

Table 3. Mesh type in mesh sensitivity study.

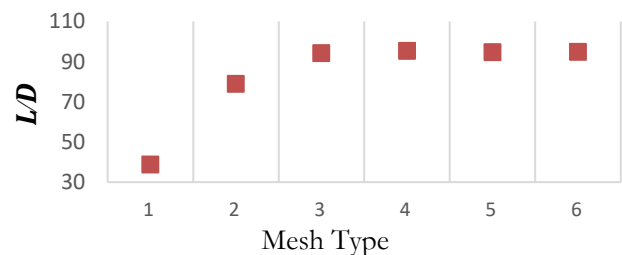| Mesh Type	No of Elements	C_L	C_D	L/D
1	18158	1.3577	0.0349	38.86
2	26060	1.3936	0.0177	78.92
3	34217	1.3882	0.0147	94.26
4	40197	1.3851	0.0145	95.36
5	57598	1.3833	0.0146	94.75
6	60485	1.3875	0.0146	94.87

Fig. 7. Comparison of L/D obtained from different mesh types.

Figure 7 shows lift-to-drag ratio values obtained with six different meshes. It is clearly shown that the element number has a great effect on the prediction. The larger the element number is, the more accurate the value. When the element number is too small, it will generate an inaccurate result and it will take more time when the element number is too large. That is the main reason for the mesh sensitivity study. It can enable the study to achieve an accurate solution with a mesh that is sufficiently dense and not overly demanding of computing resources. The change in lift-to-drag ratio becomes insignificant between

mesh type 5 to 6. So, mesh type 5 was used to reduce the simulation time.

4.3. Model Setup

A numerical scheme based on the standard k-epsilon turbulence model, generalized the finite volume method and the steady two-dimensional incompressible Navier-Stokes equations was used with the standard wall functions. The velocity inlet and pressure outlet were set up. All other boundaries including the airfoil surface are assigned as a no-slip stationary wall boundary condition. In the flow solver, a pressure-velocity coupling was used. The simulations are considered to converge when the differences between the values of the residuals are lower than 10^{-3} and the differences for the coefficients are lower than 10^{-5}. Both the residuals and the coefficients are monitored and checked while running. The converged steady state results were obtained after approximately 300 iterations. The results of the CFD simulations are the aerodynamic coefficients. Lists of the input data and settings for these airfoil simulations shown in Table 4.

Table 4.   Flow model used in Ansys Fluent.

General	Pressure based with absolute velocity formulation
Time	Steady with 2D Space Planner
Model (Viscous)	Realizable k-epsilon with Standard wall Functions
Material	Air
Boundary Condition	Velocity Inlet, Pressure Outlet & Wall
Velocity	30 m/s = 108 km/hr
Solution Method	Coupled

4.4. Validation

In our research, a numerical tool using Ansys Fluent was used to simulate the NACA 4412 airfoil both in ground effect and unbounded condition. A validation process was performed before analyzing the results obtained from the CFD simulations to make sure the model used can generate acceptable results. The results were compared to a set of established data [31]. We compared the results based on the angle of attack variation in ground effect and find agreement with those published [31]. Both the simulated results and the published data are calculated with various ground clearances and angles of attack. The simulation results for the present experiment utilized the above settings, and the percent errors were calculated by comparing with the published data [31]. The comparison results of lift and drag coefficient presented in Tables 5 and 6, respectively. The percent error for the lift coefficient remains under 4% and it is within 17% for the drag coefficient. The simulation model we created gives an acceptable result.

Table 5.   % Error for C_L.

H/C	AoA	2006 (A. Firooz)	Present Simulation	% Error
0.1	4	1.0707	1.0651	0.53
0.2	4	0.9824	1.0005	1.81
0.3	4	0.9366	0.9679	3.24
0.5	4	0.9143	0.9371	2.44
0.8	4	0.8957	0.9177	2.40
0.1	6	1.2667	1.2625	0.34
0.2	6	1.1705	1.2060	2.95
0.3	6	1.1346	1.1741	3.37
0.5	6	1.1073	1.1462	3.39
0.8	6	1.1016	1.1311	2.61
0.1	8	1.4331	1.4252	0.55
0.2	8	1.3427	1.3833	2.93
0.3	8	1.3098	1.3568	3.47
0.5	8	1.2895	1.3405	3.81
0.8	8	1.2847	1.3326	3.59

Table 6.   % Error for C_D.

H/C	AoA	2006 (A. Firooz)	Present Simulation	% Error
0.1	4	0.0103	0.0100	3.11
0.2	4	0.0108	0.0105	2.33
0.3	4	0.0110	0.0110	0.22
0.5	4	0.0117	0.0119	2.08
0.8	4	0.0124	0.0133	6.49
0.1	6	0.0117	0.0119	1.52
0.2	6	0.0124	0.0121	2.34
0.3	6	0.0127	0.0128	0.56
0.5	6	0.0127	0.0139	8.66
0.8	6	0.0137	0.0155	11.76
0.1	8	0.0131	0.0145	9.93
0.2	8	0.0145	0.0146	1.17
0.3	8	0.0141	0.0153	7.63
0.5	8	0.0145	0.0167	13.38
0.8	8	0.0158	0.0189	16.31

5. Results

In this numerical investigation, CFD computations were used to examine the varieties of lift coefficient and drag coefficient versus ground clearance and AoA. The results from the 9 simulations, arranged by 3^k full factorial design of experiments are shown in Table 7.

Table 7.   Results from Simulation.

cc	H/C	AoA	C_L	C_D	L/D	C_M
1	0.10	4	1.0651	0.0100	106.51	-0.1419
2	0.15	4	1.0267	0.0102	100.66	-0.1393
3	0.20	4	1.0005	0.0105	95.29	-0.1369
4	0.10	6	1.2625	0.0119	106.09	-0.1859
5	0.15	6	1.2310	0.0120	102.58	-0.1864
6	0.20	6	1.2060	0.0121	99.67	-0.1856
7	0.10	8	1.4252	0.0145	98.29	-0.2245
8	0.15	8	1.4007	0.0145	96.60	-0.2300
9	0.20	8	1.3833	0.0146	94.75	-0.2298

Figures 8 and 9 show two-dimensional results for the airfoil near the ground. The lift curves show the trend that lift coefficients decrease with respect to ground clearance increments. However, the drag curves indicate drag coefficients increase at that time. As a result, lift-to-drag ratio will decrease as the ground clearance increases. While the angle of attack increases, both lift coefficient and drag coefficient increase, resulting in a decline of lift-to-drag ratio: the higher the ground clearance, the lower the lift-to-drag ratio. This is because the ground effect caused by the presence of a boundary at small distances below the airfoil increases as the ground clearance decreases. When the airfoil is far from the ground, the boundary results in the flow around the airfoil being altered which causes a decrease of pressure below, reducing lift-to-drag ratio. It shows the effectiveness of ground clearance and angle of attack.
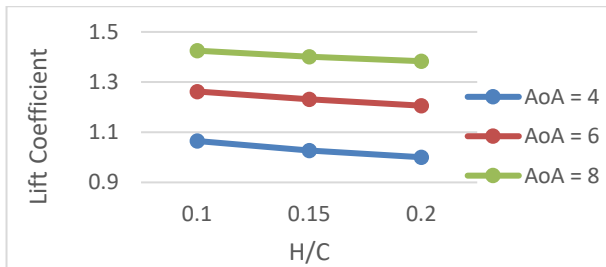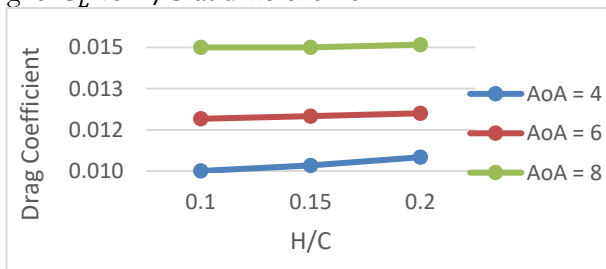

Fig. 8. C_L vs H/C at different AoA.
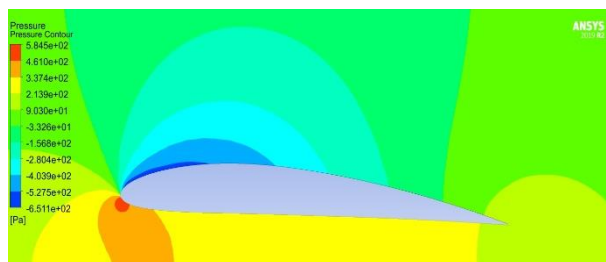

Fig. 9. C_D vs H/C at different AoA.

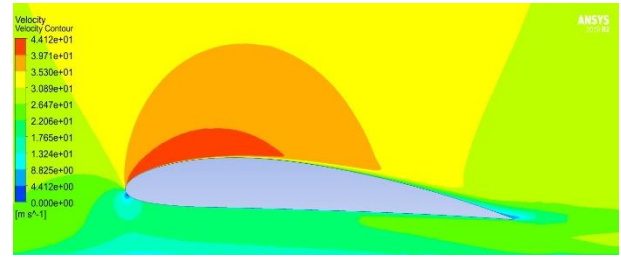Fig. 10. Pressure Contours at AoA = 4 & H/C = 0.1.

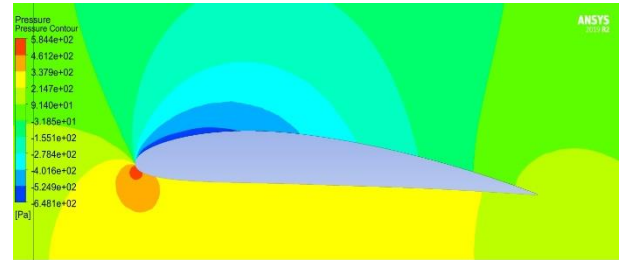Fig. 11. Velocity Contours at AoA = 4 & H/C = 0.1.

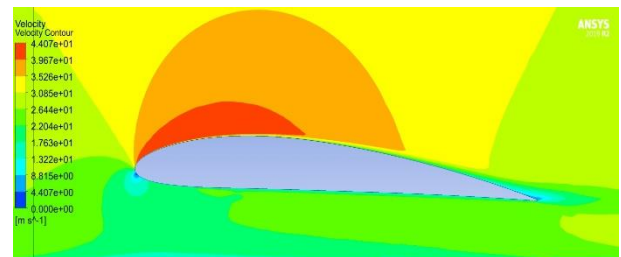Fig. 12. Pressure Contours at AoA = 4 & H/C = 0.15.

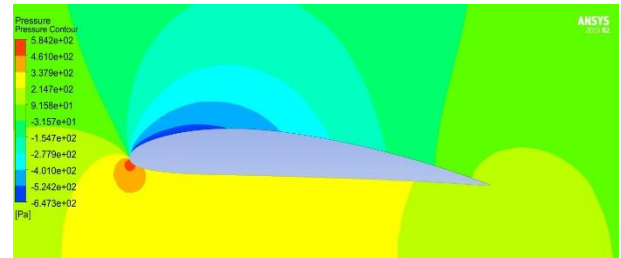Fig. 13. Velocity Contours at AoA = 4 & H/C = 0.15.

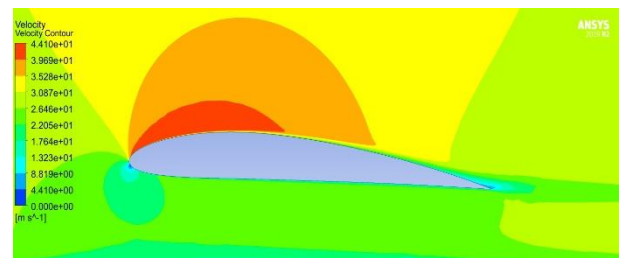Fig. 14. Pressure Contours at AoA = 4 & H/C = 0.2.

Fig. 15. Velocity Contours at AoA = 4 & H/C = 0.2.

Figures 10 to 15 show the simulation outcomes of static pressure and velocity contours at angles of attack 4°, 6° and 8° at 0.1, 0.15 and 0.2 ground clearance. From the contours, we can see that we have low pressure whenever there is low velocity and vice versa as we know from the Bernoulli equation. There is a region of low pressure on the upper surface of the airfoil and high-pressure regions at the leading edge and the lower surface of the airfoil. As a result, this pressure difference pushes the airfoil upward.

6. Analysis

Since the variation of the two factors is arranged with 3^k full factorial design of experiments, the Analysis of Variance was carried out to identify the more significant parameters from these two effects, and their effectiveness.

Further analysis, such as main effect plot and interaction plot was carried out using Minitab. After identifying the significant parameters, the regression model of the lift-to-drag ratio can be generated.

6.1. Analysis of Variance (ANOVA) for Lift-to-Drag Ratio

ANOVA is used to analyze the results and generate the main effect plots. From the plots, the most important parameter which affects the aerodynamic efficiency can be identified. The optimized values of the parameters can be obtained from regression with surface and contour plots. In this study, the significant level $\alpha = 0.05$ has been selected. The result of ANOVA for L/D is summarized in Table 8.

Table 8.   Results of ANOVA for L/D.

Source	DF	Adj SS	Adj MS	F-Value	P-Value
Model	4	136.47	34.117	10.02	0.023
Linear	4	136.47	34.117	10.02	0.023
H/C	2	76.83	38.416	11.28	0.023
AoA	2	59.64	29.818	8.76	0.035
Error	4	13.62	3.405		
Total	8	150.09			

The normal probability plot in Fig. 16 shows that the error is normally distributed. In the residuals versus fits plot, the residuals are randomly distributed showing constant variance. The residuals drop randomly around the center line on the residuals versus order plot indicating the residuals independency.
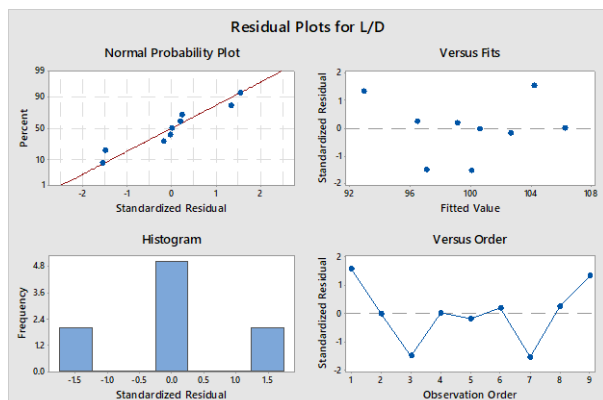

Fig. 16. Residual plots for L/D deviation.

6.1.1. Main and interaction effects

The main effect of both H/C (factor A) and AoA (factor B) are statistically significant at 95% confidence. Factor B has a slight rise period first. It drastically drops down after that. Both factors have a negative standardized effect, meaning that the lift-to-drag ratio will decrease when factor A or B increases. This can be seen from the main effect plots (Fig. 17).
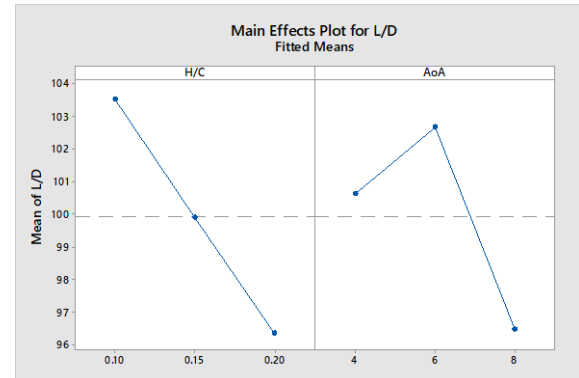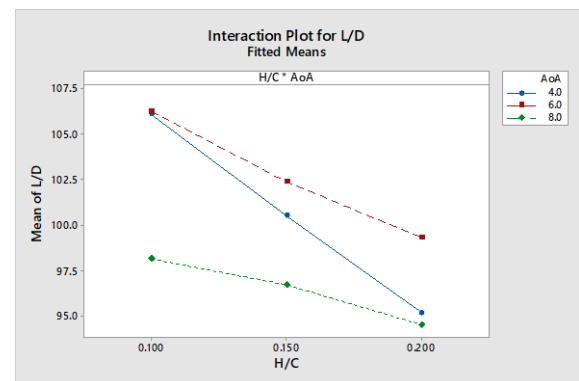

Fig. 17. Main Effect Plot for L/D.

Fig. 18. Interaction Plot for L/D.

The lines which have no crossing point on the interaction plot (Fig. 18) show that there is no interaction effect between A and B, which is confirmed with the Pareto chart of the standardized effects (Fig. 19)
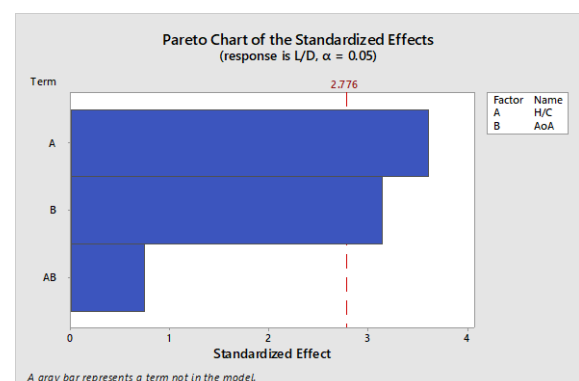

Fig. 19. Pareto chart of the standardized effects for L/D.

6.1.1 Regression model

Since there is no interaction between the two factors, we exclude this interaction from the model. The regression model is stated as below.

$$L/D = 116.86 - 71.6\,H/C - 1.033\,AoA \qquad (1)$$

Table 9. Results of ANOVA of the fitted regression for L/D.

Source	DF	Adj SS	Adj MS	F-Value	P-Value
Model	2	102.44	51.222	6.45	0.032
H/C	1	76.83	76.827	9.67	0.021
AoA	1	25.62	25.617	3.23	0.123
Error	6	47.64	7.941		
Total	8	150.09			

With the new fitted regression in Eq. (1), the ANOVA results are summarized in Table 9 and the new residual plots are shown in Fig. 20.
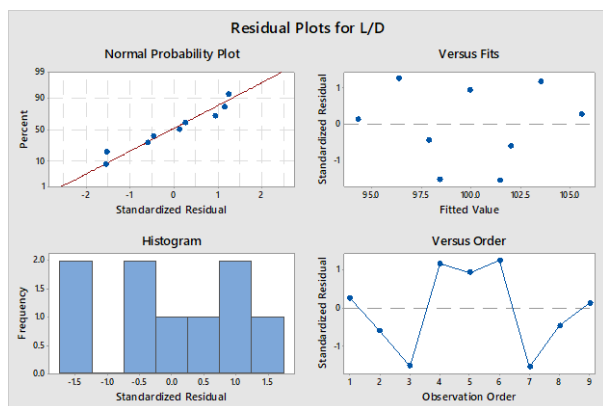

Fig. 20. Residual plots for L/D deviation of the fitted regression.

After fitting the regression model, R-squared is checked to determine how well the model fits the data. It measures the strength of the relationship between the model and the dependent variable on a convenient 0 to 100% scale. For our model of lift-to-drag ratio, R-squared value is 92.25% meaning that the model we produced can give a result which is 92.25% accurate.

6.1.2. Response surface

The response surface plot and contour plot of L/D deviation as a function of ground clearance and angle of attack are established from Eq. (1) as shown in Fig. 21 & 22. A three-dimensional view of the surface plot provides a clearer picture of the response (Fig. 21). In the contour plot, the response surface is displayed as a two-dimensional plane in which all points with the same response are connected to produce contour lines with a constant response (Fig. 22). Both contour and surface plots help to understand the nature of the relationship

between the two factors (ground clearance and angle of attack) and the response (lift-to-drag ratio). As can be seen in Fig. 21 & 22, the ratio increases with a decrease in both ground clearance and angle of attack.
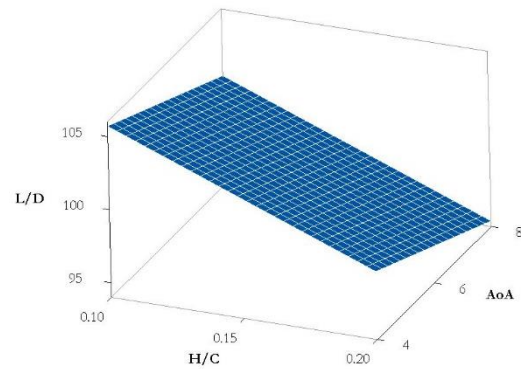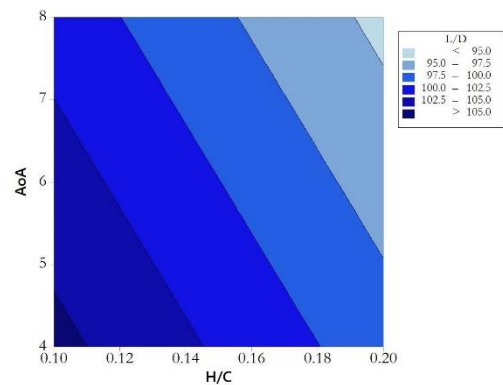

Fig. 21. Response Surface for L/D.

Fig. 22. Contour Plot for L/D.

6.2. Analysis of Variance (ANOVA) for Moment Coefficient

The result of ANOVA for moment coefficient is summarized in Table 10.

Table 10. Results of ANOVA for moment coefficient.

Source	DF	Adj SS	Adj MS	F-Value	P-Value
Model	4	0.0117	0.0029	429.27	0.0000
Linear	4	0.0117	0.0029	429.27	0.0000
H/C	2	0.0000	0.0000	0.06	0.9450
AoA	2	0.0117	0.0058	858.49	0.0000
Error	4	0.0000	0.0000		
Total	8	0.0117			

In Fig. 23, the residual plots show the normal distribution of error with constant variance.
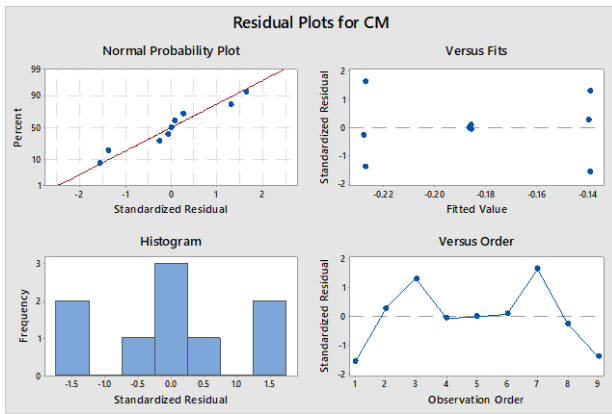
Fig. 23. Residual plots for moment coefficient.

6.2.1. Main and interaction effects

The main effect of AoA (factor B) only is statistically significant at 95% confidence. Factor B has a negative standardized effect, meaning that moment coefficient will decrease when factor B increases. It can be seen from the main effect plots (Fig. 24). From the interaction plot (Fig. 25), the parallel lines show that there is no interaction effect between A and B. This is also confirmed by the Pareto chart of the standardized effects (Fig. 26)
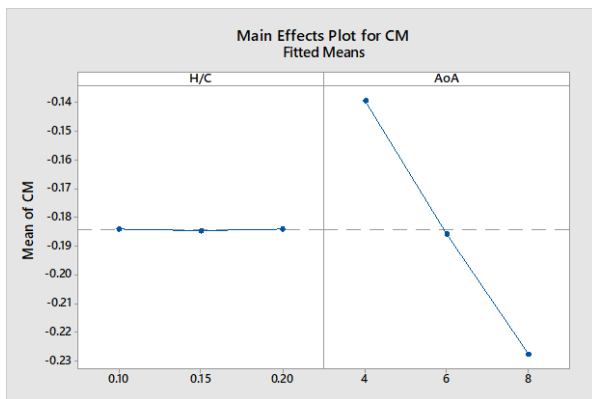

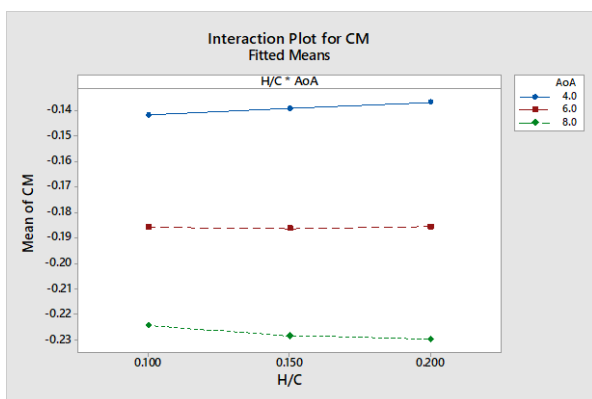Fig. 24. Main Effect Plot for moment coefficient.
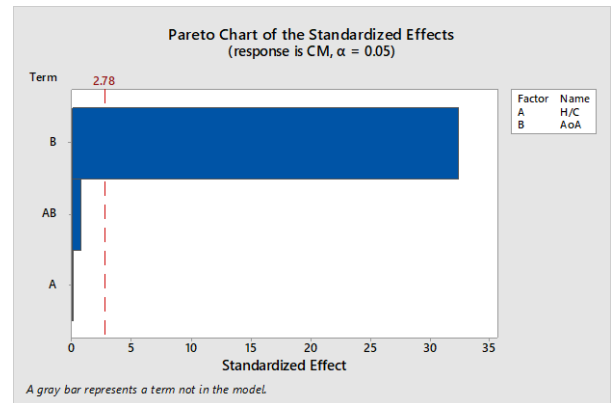

Fig. 25. Interaction Plot for moment coefficient.

Fig. 26. Pareto chart of the standardized effects for moment coefficient.

6.2.2. Regression model

The P-Value of factor A is higher than 0.05 and there is no interaction between the two factors. We exclude factor A and the interaction from the model. The regression model is stated as below.

$$C_M = -0.05201 - 0.022047\,AoA \qquad (2)$$

Table 11. Results of ANOVA of the fitted regression for moment coefficient.

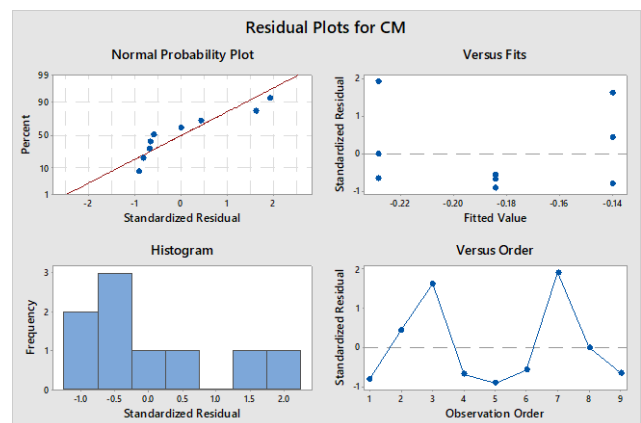| Source	DF	Adj SS	Adj MS	F-Value	P-Value
Regression	1	0.0117	0.0117	2006	0.00
AoA	1	0.0117	0.0117	2006	0.00
Error	7	0.0000	0.0000		
Lack-of Fit	1	0.0000	0.0000	3	0.15
Pure Error	6	0.0000	0.0000		
Total	8	0.0117			

Fig. 27. Residual plots for moment coefficient of the fitted regression.

From Eq. (2), the ANOVA results of the fitted regression for the moment coefficient are obtained as presented in Table 11 and the new residual plots are shown in Fig. 27. The resulting R-squared value is 99.65%.

6.2.3. Response surface

Response plot of moment coefficient as a function of angle of attack from Eq. (2) is presented in Fig. 28. In this plot, the response appears as a line with one variable in the regression model. The relationship of the moment coefficient and angle of attack can be seen from the graph.
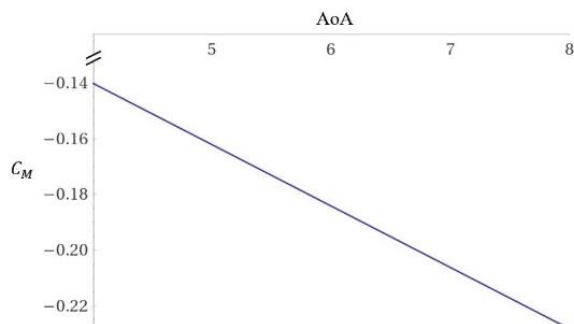

Fig. 28. Response Plot for Moment Coefficient.

7. Conclusion

NACA4412 airfoil numerical experiments on ground effect and angle of attack dispersion are performed to facilitate understanding of ground effects and to test their effectiveness against aerodynamic factors. The experimental plan is constructed based on the three-level factorial design of experiments to be able to develop a regression model for lift-to-drag ratio as a response. It states that there is no interaction between these two factors, ground clearance and angle of attack for both lift-to-drag ratio and moment coefficient. Both factors produce a negative effect on the lift-to-drag ratio. If the values are higher, the ratio will be lower. For the moment coefficient, the negative effect of factor B is significant. However, this only confirms the limits investigated. From the regression model, we can find the optimum lift-to-drag ratio and moment coefficient within 0.1 to 0.2 ground clearance and from 4 to 8 angle of attack at velocity of 30 m/s. It is helpful to estimate the value when designing and testing the NACA 4412 airfoil within these limits. Beyond the limits, the regression models will not give accurate results. More experiments are needed to expand the limitations, such as more various angles of attack, ground clearance and flow velocity. Although there is much research about the airfoil out of ground effect, research on ground effects is still limited. For Wing in Ground Effect (WIG) craft development, aerodynamic investigation of the airfoil in ground effect is the foundation. Researchers need to create a stronger foundation by expanding the limitations of the current research.

References

[1] K. V. Rozhdestvensky, "Wing-in-ground effect vehicles," *Progress in Aerospace Sciences,* vol. 42, no. 3, pp. 211-283, May 2006.

[2] I. A. Amin, "Efficiency of wing-in-ground marine crafts," Ph.D. thesis, Department of Naval Architecture and Marine Engineering, Port Said University, Port Said, Egypt, 2006.

[3] M. Halloran, "Wing in ground effect craft review," Aeronautical and Maritime Research Laboratory, Department of Defence Science & Technology Organization, Melbourne Victoria, Australia, 1999.

[4] S. Kandasamy, N. K. Sinha, and J. Umakanth, "Parametric optimization of high aspect ratio wing using surrogate model," *IFAC-PapersOnLine*, vol. 51, no. 1, pp. 231-236, January 2018.

[5] H. Hameed, "The design of a four-seat reverse delta WIG craft," *The Maldives National Journal of Research,* vol. 7, No. 1, pp. 7-28, December 2019.

[6] S. Wiriadidjaja, Z. Mohamad, A. Rafie, M. Elhadi, A. Fariduzzaman, and F. Hasim, "Wing-in-ground-effect craft as a potential domestic transport vehicle," in *34th AIAA Applied Aerodynamics Conference*, Washington, D.C., 2016.

[7] C. Erjie and Z. Xin, "Ground effect aerodynamics," in *Incompressible Flows and Aerodynamics*. John Wiley & Sons, Ltd., 2010.

[8] J. D. Anderson, *Fundamentals of Aerodynamics*, 5th ed. McGraw-Hill, 2010.

[9] R. Ranzenbach and J. Barlow, "Two-dimensional airfoil in ground effect, An experimental and computational study," in *Motorsports Engineering Conference & Expostion*, 1994.

[10] M. D. Hossain and M. F. Raiyan, "A comparative flow analysis of NACA 6409 and NACA 4412 aerofoil," *International Journal of Research in Engineering and Technology,* vol. 03, pp. 342-350, October 2014.

[11] M. R. Ahmed, "Flow over thick airfoils in ground effect—An investigation on the influence of camber," in *24th International Congress of the Aeronautical Sciences*, 2004.

[12] M. R. Ahmed and S. D. Sharma, "An investigation on the aerodynamics of a symmetrical airfoil in ground effect," *Experimental Thermal and Fluid Science,* vol. 29, pp. 633-647, February 2005.

[13] M. R. Ahmed, "Aerodynamics of a cambered airfoil in ground effect," *International Journal of Fluid Mechanics Research,* vol. 32, pp. 157-183, January 2005.

[14] H. Chih-Min and G. Cha'o-Kuang, "Aerodynamic characteristics of a two-dimensional airfoil with ground effect," *Journal of Aircraft,* vol. 33, pp. 386-392, March 1996.

[15] M. R. Ahmed, T. Takasaki, and Y. Kohama, "Aerodynamics of a NACA4412 airfoil in ground effect," *AIAA Journal,* vol. 45, pp. 37-47, January 2007.

[16] M. R. Ahmed, T. Takasaki, and Y. Kohama, "Experiments on the aerodynamics of a cambered airfoil in ground effect," in *44th AIAA Aerospace Sciences Meeting and Exhibit*, Reno, Nevada, 2006.

[17] Q. Qu, Z. Lu, P. Liu, and R. Agarwal, "Numerical study of aerodynamics of a wing-in-ground-effect

craft," *Journal of Aircraft,* vol. 51, pp. 913-924, May 2014.

[18] I. H. Abbott and A. E. Von Doenhoff, *Theory of Wing Sections*. Dover Publications, 1959.

[19] *NACA 4412 Coordinate.* [Online]. Available: http://www.airfoiltools.com (accessed Jan. 31, 2020).

[20] D. C. Montgomery, *Design and Analysis of Experiments*, 8th ed. John Wiley & Sons, Inc., 2012.

[21] C. Victoria, T. Kwok-Leung, R. B. Russell, and K. A. Janet, "A review of design and modelling in computer experiments," in *Handbook of Statistics*. Elsevier, 2003, pp. 231-261.

[22] M. Uy and J. K. Telford, "Optimization by design of experiment techniques," in *2009 IEEE Aerospace Conference*, Big Sky, Montana, 2009.

[23] K. S. Milani, M. Mamourian, S. Mirzakhanlari, R. Ellahi, and K. Vafai, "Numerical investigation and sensitivity analysis of effective parameters on combined heat transfer performance in a porous solar cavity receiver by response surface methodology," *International Journal of Heat and Mass Transfer,* vol. 105, pp. 811-825, 2017.

[24] S. Güngör, U. Ceyhan, and Z. H. Karadeniz, "Optimization of heat transfer in a grooved pipe model by Stochastic Algorithms and DOE based RSM," *International Journal of Thermal Sciences,* vol. 159, 2021.

[25] M. Thianwiboon, "Parameter tuning of the autonomous boat in fish farming industry with design of experiment," *Engineering Journal*, vol. 24, no. 5, pp. 217-225, September 2020.

[26] R. Yondo, E. Andrés, and E. Valero, "A review on design of experiments and surrogate models in aircraft real-time and many-query aerodynamic analyses," *Progress in Aerospace Sciences,* vol. 96, pp. 23-61, 2018.

[27] M. Altekar, C. A. Homon, M. A. Kashem, S. W. Mason, R. M. Nelson, L. A. Patnaude, J. Yingling, and P. B. Taylor, "Assay optimization: A statistical design of experiments approach," *Clin Lab Med,* vol. 27, no. 1, pp. 139-54, March 2007.

[28] Z. Li and X. Zheng, "Review of design optimization methods for turbomachinery aerodynamics," *Progress in Aerospace Sciences,* vol. 93, pp. 1-23, 2017.

[29] A. Sadikin, "A comparative study of turbulence models on aerodynamics characteristics of a NACA0012 airfoil," *International Journal of Integrated Engineering,* vol. 10, no. 1, 2018.

[30] ANSYS, *ANSYS Fluent User's Guide*. ANSYS, Inc., 2013.

[31] A. Firooz and M. Gadami, "Turbulence flow for NACA 4412 in unbounded flow and ground effect with different turbulence models and two ground conditions: Fixed and moving ground conditions," in *Int. Conference on Boundary and Interior Layers*, Goettingen, Germany, 2006.

———— • ————

Shwe Yee Win was born in Myinmu, Myanmar in 1994. She received the B.E. degree in Mechanical Precision & Automation engineering from the University of Technology, Yatanarpon Cyber City, Myanmar, in 2015.

Her research interests are in the field of aerodynamics and computational fluid dynamics.

Mongkol Thianwiboon was born in Lampang, Thailand in 1976. He received the B.S. and M.S. and the Ph.D. degrees in mechanical engineering from Chulalongkorn University in 1997, 2000 and 2005 respectively.

From 2000 to 2005, he was a system administrator at the Engineering Computer Center, Chulalongkorn University while studying the Ph.D. degree. After that, he worked with Lenso Wheel Co., Ltd as a project engineer from 2005 to 2008. Later, he was the manager of the Process Improvement Department from 2008 to 2011. Since 2011, he has been a faculty member of the Industrial Engineering Department, Mahidol University. His research interests include robotic and autonomous systems and computational fluid dynamics.

Dr. Thianwiboon is a member of the Council of Engineers and Society of Automotive Engineers - Thailand (TSAE).